Computational Mathematics and Modeling, Vol. 25, No. 3, July, 2014

PERISTALTIC FLOW OF VISCOUS FLUID IN A RECTANGULAR DUCT WITH COMPLIANT WALLS

S. Nadeem,[1] Arshad Riaz,[1] and R. Ellahi[2]

In the present article, we have examined the peristaltic flow of a viscous fluid in a rectangular channel with compliant walls. The long wavelength and low Reynolds number approximations are employed to simplify the governing equations. The reduced linear nonhomogeneous partial differential equations are solved by using the eigenfunction expansion method. The physical features of pertinent parameters have been discussed by plotting graphs of velocity for both two-dimensional and three-dimensional cases. The trapping phenomenon is also discussed.

Keywords: Peristaltic flow, viscous fluid, rectangular duct, compliant walls, analytical solution.

Introduction

Peristaltic flows have permanent importance in physiology and other biosciences. The occurrence of such flows is quite prevalent in nature; in particular, these flows are encountered in smooth muscle contraction. Because of their importance, a number of researchers are engaged in this rich area; they present the peristaltic flows theoretically, experimentally and numerically keeping different flow geometries. Some recent studies of peristaltic flows with different flow geometries are given in [1–8]. Each physical geometry of peristaltic flows requires different physical experiments and has different meanings. The mathematical model of peristaltic flow in a two-dimensional symmetric and asymmetric channel was discussed by Eytan and Elad [10] as applied to interuterine fluid flow in a nonpregnant uterus. Some recent studies of Reddy et al. [11] and Nadeem and Akram [12] showed that the sagittal cross section of the uterus may be better approximated by a tube of rectangular cross section than a two-dimensional channel. The influence of heat and mass transfer on MHD peristaltic flow through a porous space with compliant walls has been discussed by Srinivas and Kothandapani [13]. However, the peristaltic flow in a rectangular channel with compliant walls is still unexplored. The aim of the present paper is to provide a new concept on the peristaltic flow of a viscous fluid in a rectangular channel having compliant walls. The governing equations and the boundary conditions are simplified under the assumptions of long wavelength and low Reynolds number. The exact solution of the reduced problem has been found with the help of the eigenfunction expansion method. The physical features of pertinent parameters are discussed through graphs of velocity and stream functions. The three-dimensional behavior of velocity is also presented through graphs.

Mathematical Formulation

Consider the peristaltic flow of an incompressible viscous fluid in a duct of rectangular cross section having channel width $2d$ and height $2a$. We are considering the Cartesian coordinate system in a such way that the x

[1] Department of Mathematics, Quaid-i-Azam University 45320, Islamabad 44000 Pakistan; e-mail: snqau@hotmail.com.

[2] Department of Mathematics and Statistics, FBAS, IIU, Islamabad, 44000, Pakistan.

 1046–283X/14/2503–0404

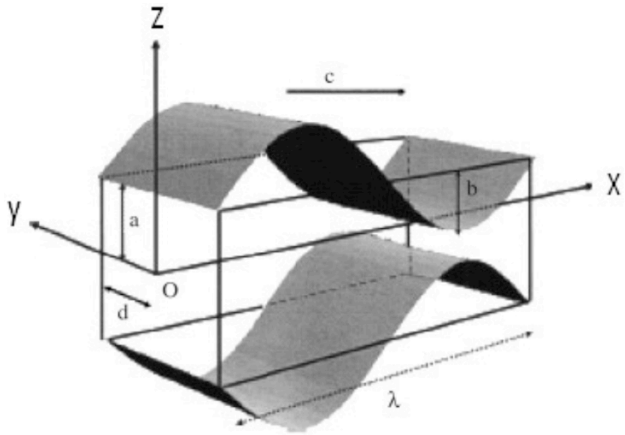

Fig. 1. Schematic diagram for peristaltic flow in a rectangular duct.

axis is taken along the axial direction, the y axis is taken along the lateral direction, and the z axis is along the vertical direction of the rectangular channel. The walls of the channel are assumed to be flexible and are taken as compliant, on which waves with small amplitude and long wavelength are considered.

The geometry of the channel wall is given by

$$z = h(x,t) = \pm a \pm b \cos\left[\frac{2\pi}{\lambda}(x - ct)\right],$$

where a and b are the amplitudes of the waves, λ is the wavelength, c is the velocity of propagation, t is the time, and x is the direction of wave propagation. The walls parallel to xz plane remain undisturbed and are not subject to any peristaltic wave motion. We assume that the lateral velocity is zero as there is no change in lateral direction of the duct cross section. Let $(u,0,w)$ be the velocity for a rectangular duct. The governing equations for the flow problem are stated as

$$\frac{\partial u}{\partial x} + \frac{\partial w}{\partial z} = 0\,, \tag{1}$$

$$\rho\left(\frac{\partial u}{\partial t} + u\frac{\partial u}{\partial x} + w\frac{\partial u}{\partial z}\right) = -\frac{\partial p}{\partial x} + \mu\left(\frac{\partial^2 u}{\partial x^2} + \frac{\partial^2 u}{\partial y^2} + \frac{\partial^2 u}{\partial z^2}\right), \tag{2}$$

$$0 = -\frac{\partial p}{\partial y}, \tag{3}$$

$$\rho\left(\frac{\partial w}{\partial t} + u\frac{\partial w}{\partial x} + w\frac{\partial w}{\partial z}\right) = -\frac{\partial p}{\partial z} + \mu\left(\frac{\partial^2 w}{\partial x^2} + \frac{\partial^2 w}{\partial y^2} + \frac{\partial^2 w}{\partial z^2}\right), \tag{4}$$

in which ρ is the density and p is the pressure. Let us define the following nondimensional quantities

$$\bar{x} = \frac{x}{\lambda}, \quad \bar{y} = \frac{y}{d}, \quad \bar{z} = \frac{z}{a}, \quad \bar{u} = \frac{u}{c}, \quad \bar{w} = \frac{\lambda w}{ca}, \quad \bar{t} = \frac{ct}{\lambda}, \quad \bar{h} = \frac{h}{a}, \quad \bar{p} = \frac{a^2 p}{\mu c \lambda},$$

$$\mathrm{Re} = \frac{\rho a c}{\mu}, \quad \delta = \frac{a}{\lambda}, \quad \varphi = \frac{b}{a}, \quad \beta = \frac{a}{d}.$$

Using the above nondimensional quantities in Eqs. (1) to (4), we write the resulting equations (after dropping the bars) as

$$\frac{\partial u}{\partial x} + \frac{\partial w}{\partial z} = 0, \tag{5}$$

$$\mathrm{Re}\,\delta\left(\frac{\partial u}{\partial t} + u\frac{\partial u}{\partial x} + w\frac{\partial u}{\partial z}\right) = -\frac{\partial p}{\partial x} + \delta^2\frac{\partial^2 u}{\partial x^2} + \beta^2\frac{\partial^2 u}{\partial y^2} + \frac{\partial^2 u}{\partial z^2}, \tag{6}$$

$$0 = -\frac{\partial p}{\partial y}, \tag{7}$$

$$\mathrm{Re}\,\delta^3\left(\frac{\partial w}{\partial t} + u\frac{\partial w}{\partial x} + w\frac{\partial w}{\partial z}\right) = -\frac{\partial p}{\partial z} + \delta^2\left(\delta^2\frac{\partial^2 w}{\partial x^2} + \beta^2\frac{\partial^2 w}{\partial y^2} + \frac{\partial^2 w}{\partial z^2}\right). \tag{8}$$

Under the assumption of long wavelength $\delta \le 1$ and low Reynolds number $\mathrm{Re} \to 0$, Eqs. (6) to (8) take the form

$$\frac{\partial p}{\partial x} = \beta^2\frac{\partial^2 u}{\partial y^2} + \frac{\partial^2 u}{\partial z^2}, \tag{9}$$

$$\frac{\partial p}{\partial y} = 0, \tag{10}$$

$$\frac{\partial p}{\partial z} = 0. \tag{11}$$

The corresponding boundary conditions for compliant walls in nondimensional form are

$$u = -1 \quad \text{at} \quad y = \pm 1, \tag{12}$$

$$u = -1 \quad \text{at} \quad z = \pm h(x,t) = \pm 1 \pm \eta(x,t), \tag{13}$$

where $\eta(x,t) = \varphi\cos 2\pi(x - t)$ and $0 \le \varphi \le 1$. The governing equation for the flexible wall may be described as

$$L(\eta) = p - p_0 ,$$

where L is an operator that is used to represent the motion of a stretched membrane with viscosity damping forces such that

$$L = m\frac{\partial^2}{\partial t^2} + D\frac{\partial}{\partial t} + B\frac{\partial^4}{\partial x^4} - T\frac{\partial^2}{\partial x^2} + K.$$

In the above equation, m is the mass per unit area, d is the coefficient of the viscous damping forces, B is the flexural rigidity of the plate, T is the elastic tension per unit width in the membrane, K is the spring stiffness, and p_0 is the pressure on the outside surface of the wall due to tension in the muscle, which is assumed to be zero here. Using the continuity of stress at $z = \pm 1 \pm \eta$ and the x momentum equation, we obtain

$$\frac{\partial L(\eta)}{\partial x} = \frac{\partial}{\partial x}\left(E_1\frac{\partial^2\eta}{\partial t^2} + E_2\frac{\partial\eta}{\partial t} + E_3\frac{\partial^4\eta}{\partial x^4} - E_4\frac{\partial^2\eta}{\partial x^2} + E_5\eta \right) = \frac{\partial p}{\partial x} = \beta^2\frac{\partial^2 u}{\partial y^2} + \frac{\partial^2 u}{\partial z^2} , \tag{14}$$

where $E_1 = ma^3c/\lambda^3\mu$, $E_2 = Da^3/\mu\lambda^2$, $E_3 = Ba^3/c\mu\lambda^5$, $E_4 = Ta^3/c\mu\lambda^3$, and $E_5 = Ka^3/c\mu\lambda$ are the nondimensional elasticity parameters.

Solution of the Problem

The solution of the above boundary value problem has been computed by the eigenfunction expansion method and is directly defined as

$$u = -1 + \sum_{n=1}^{\infty}\left(1 - \frac{\cosh\lambda_n z}{\cosh\lambda_n h}\right)\frac{16C(-1)^n}{(2n-1)^3\pi^3\beta^2}\cos(2n-1)\frac{\pi}{2}y , \tag{15}$$

where

$$\lambda_n = (2n-1)\frac{\pi}{2}\beta ,$$

$$C = 2\pi\varphi\left[2E_2\pi\cos 2\pi(x-t) - \left(E_5 + 4\pi^2\left(-E_1 + E_4 + 4E_3\pi^2\right)\right)\sin 2\pi(x-t)\right].$$

Results and Discussions

In this part of the paper, the graphical results of the problem under consideration are analyzed. Figures 2–6 represent the variation of the velocity field with different values of physical parameters. The formation of an internally circulating bolus of fluid by closed streamlines is shown in Figs. 7–11. In Figs. 2–4, the velocity profile is plotted with different values of the parameters β, E_1, and E_2. From these figures, we can easily observe that the magnitude of the velocity profile is being reduced with increase in the magnitude of the above-mentioned

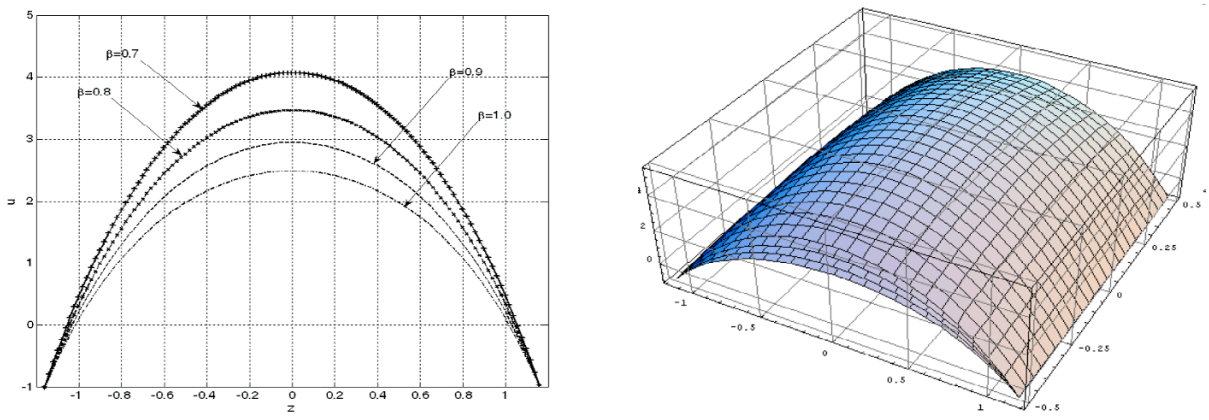

(a) **(b)**

Fig. 2. Velocity profile for different values of β for fixed $\varphi = 0.2$, $x = 0.5$, $t = 0.4$, $E_1 = 0.1$, $E_2 = 0.2$, $E_3 = 0.01$, $E_4 = 0.2$, and $E_5 = 0.3$: (a) for the 2 dimensional case, (b) for the 3 dimensional case.

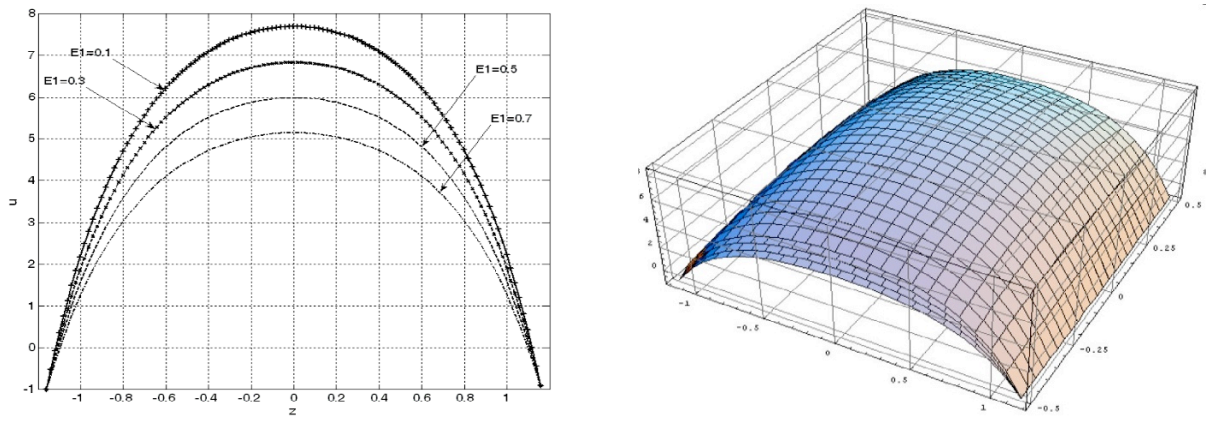

(a) **(b)**

Fig. 3. Velocity profile for different values of E_1 for fixed $\varphi = 0.2$, $x = 0.5$, $t = 0.4$, $\beta = 1.5$, $E_2 = 0.2$, $E_3 = 0.05$, $E_4 = 0.2$, and $E_5 = 0.5$: (a) for the 2 dimensional case, (b) for the 3 dimensional case.

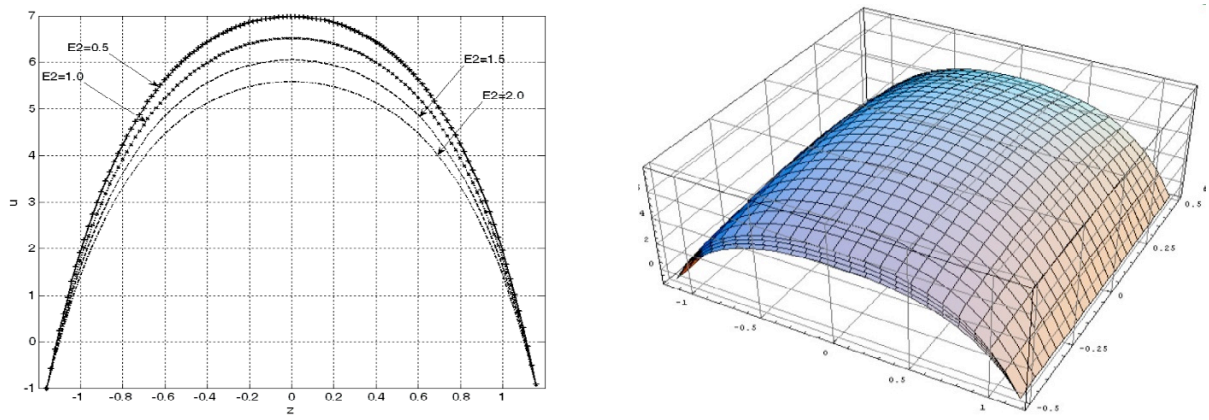

(a) **(b)**

Fig. 4. Velocity profile for different values of E_2 for fixed $\varphi = 0.2$, $x = 0.5$, $t = 0.4$, $\beta = 1.5$, $E_1 = 0.2$, $E_3 = 0.05$, $E_4 = 0.2$, and $E_5 = 0.5$: (a) for the 2 dimensional case, (b) for the 3 dimensional case.

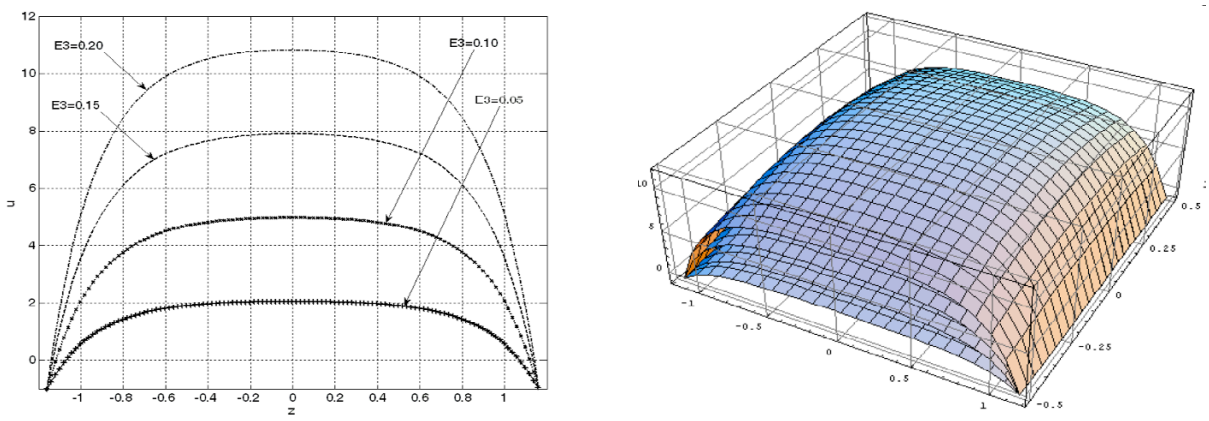

(a) **(b)**

Fig. 5. Velocity profile for different values of E_3 for fixed $\varphi = 0.2$, $x = 0.5$, $t = 0.4$, $\beta = 2.7$, $E_1 = 0.1$, $E_2 = 0.1$, $E_4 = 0.2$, and $E_5 = 0.5$: (a) for the 2 dimensional case, (b) for the 3 dimensional case.

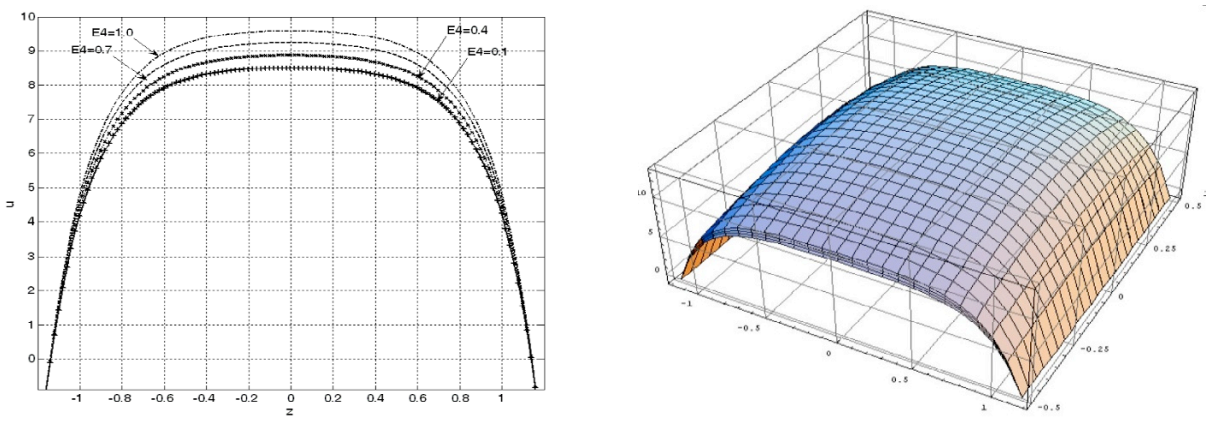

(a) **(b)**

Fig. 6. Velocity profile for different values of E_4 for fixed $\varphi = 0.2$, $x = 0.5$, $t = 0.4$, $\beta = 3$, $E_1 = 0.1$, $E_2 = 0.1$, $E_3 = 0.2$, and $E_5 = 0.5$: (a) for the 2 dimensional case, (b) for the 3 dimensional case.

parameters. The effects of different values of the physical parameters E_3 and E_4 on velocity are shown in Figs. 5 and 6. From these figures, it is easy to see that the velocity profile varies directly with E_3 and E_4. From Figs. 2–6, it can also be observed that the velocity attains its maximum value at the center of the channel. The streamlines for different values of the emerging parameters are shown in Figs. 7–11. Trapping phenomenon of the peristaltic transport can be observed from these streamlines. From Fig. 7, it is seen that the number of trapped boluses decreases with increasing magnitude of the parameter β for fixed values of the other parameters. The streamlines for different values of the parameters φ and E_1 are sketched in Figs. 8 and 9. It is observed that more trapped boluses appear with increase in the values of φ and E_1. Figure 10 highlights the streamlines for emerging parameter E_2. It is noted that the family of boluses remains the decreases with increasing E_2. From Fig. 11, we can say that the number of trapped boluses same with increasing effect of the parameters E_3, E_4, and in the left-hand side of the channel but increases in the other side. Moreover, the size of the trapped bolus also changes in the left and right side of the channel with variation of the pertinent parameters.

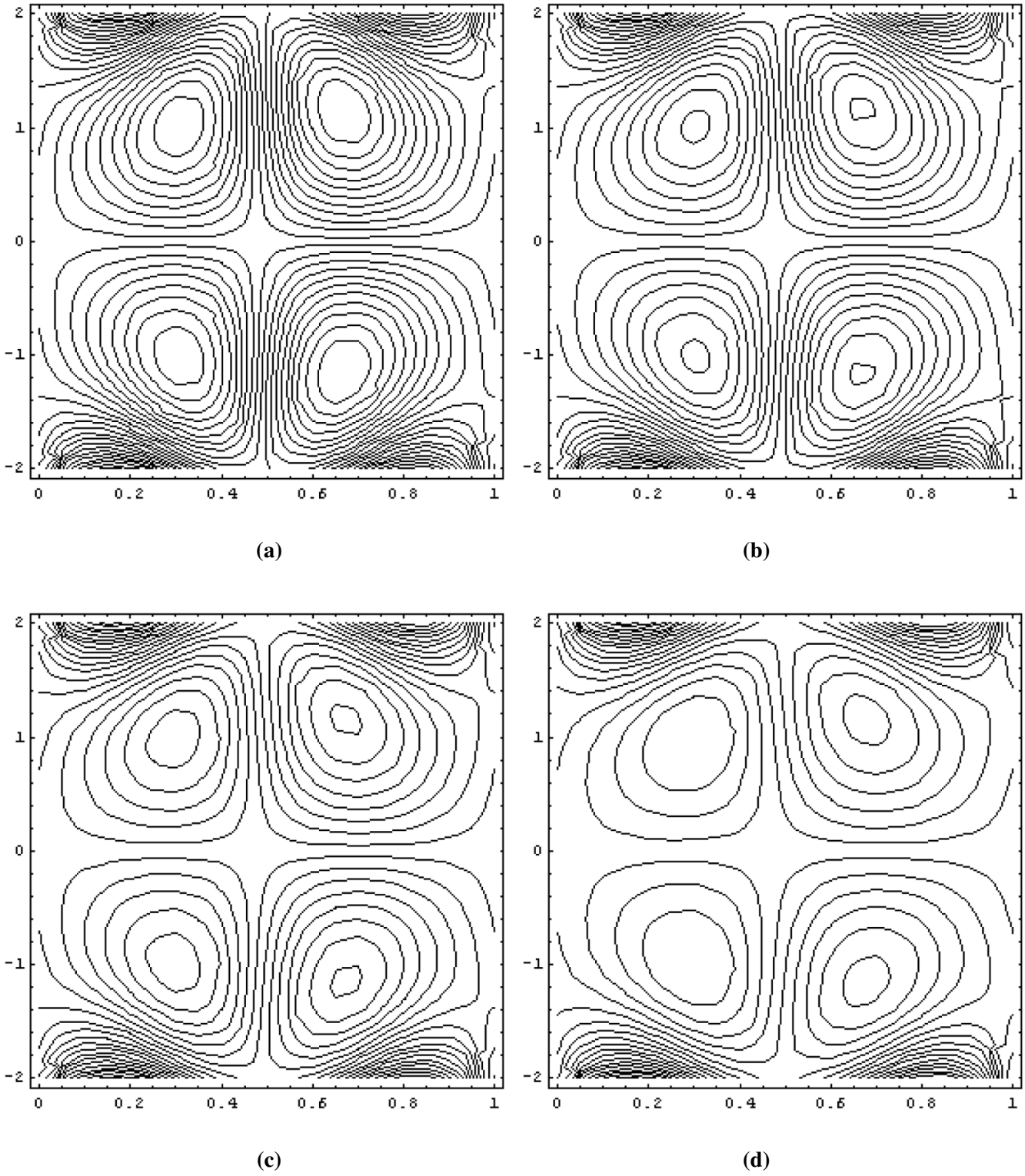

Fig. 7. Streamlines for different values of β: (a) for $\beta = 0.1$, (b) for $\beta = 0.3$, (c) for $\beta = 0.5$, (d) for $\beta = 0.7$. The other parameters are $y = 0.5$, $\varphi = 0.2$, $t = 0.5$, $E_1 = 1$, $E_2 = 0.2$, $E_3 = 0.01$, $E_4 = 0.2$, $E_5 = 0.3$.

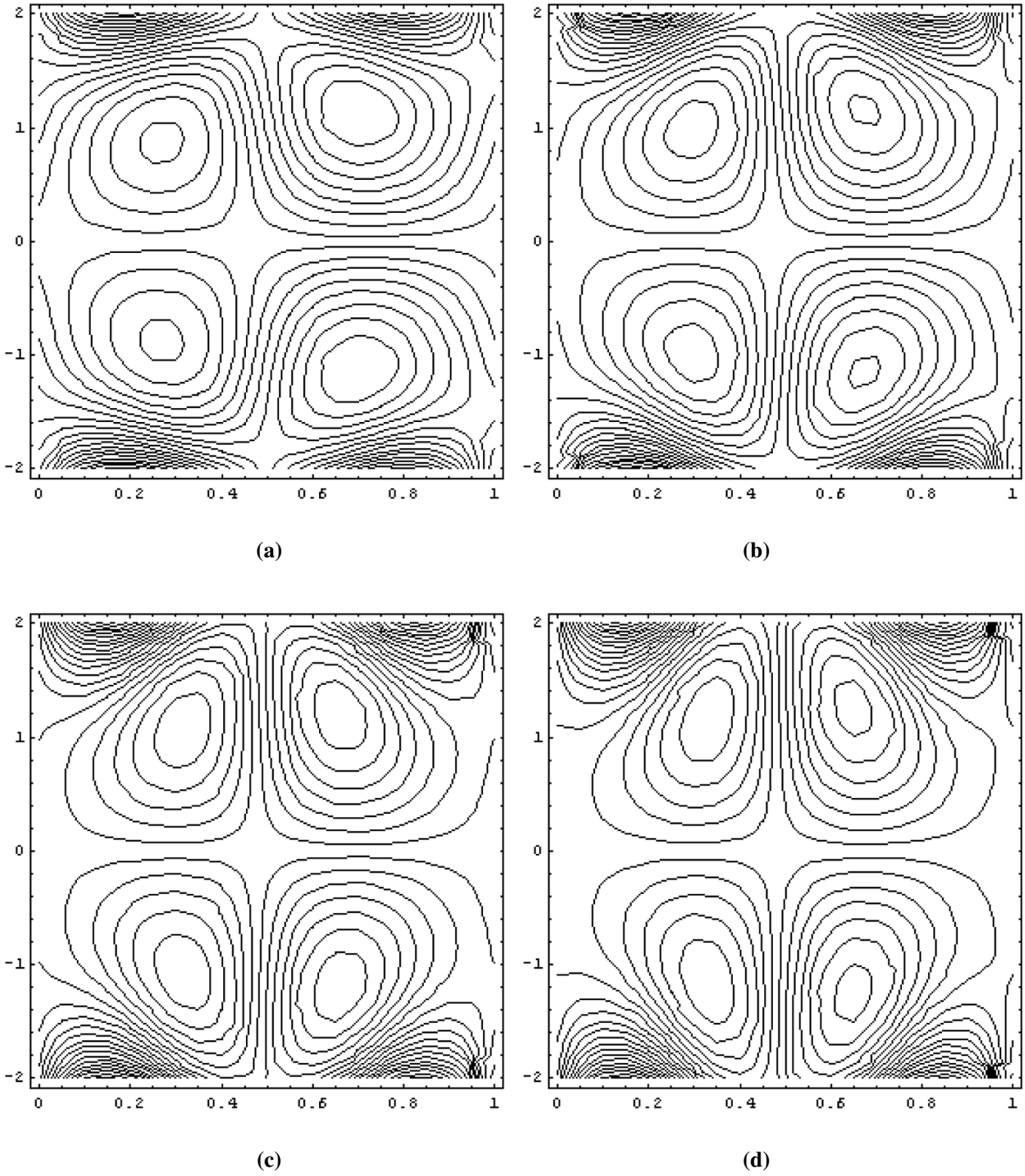

Fig. 8. Streamlines for different values of φ: (a) for $\varphi = 0.1$, (b) for $\varphi = 0.2$, (c) for $\varphi = 0.3$, (d) for $\varphi = 0.4$. The other parameters are $y = 0.5$, $\beta = 0.5$, $t = 0.5$, $E_1 = 1$, $E_2 = 0.2$, $E_3 = 0.01$, $E_4 = 0.2$, $E_5 = 0.3$.

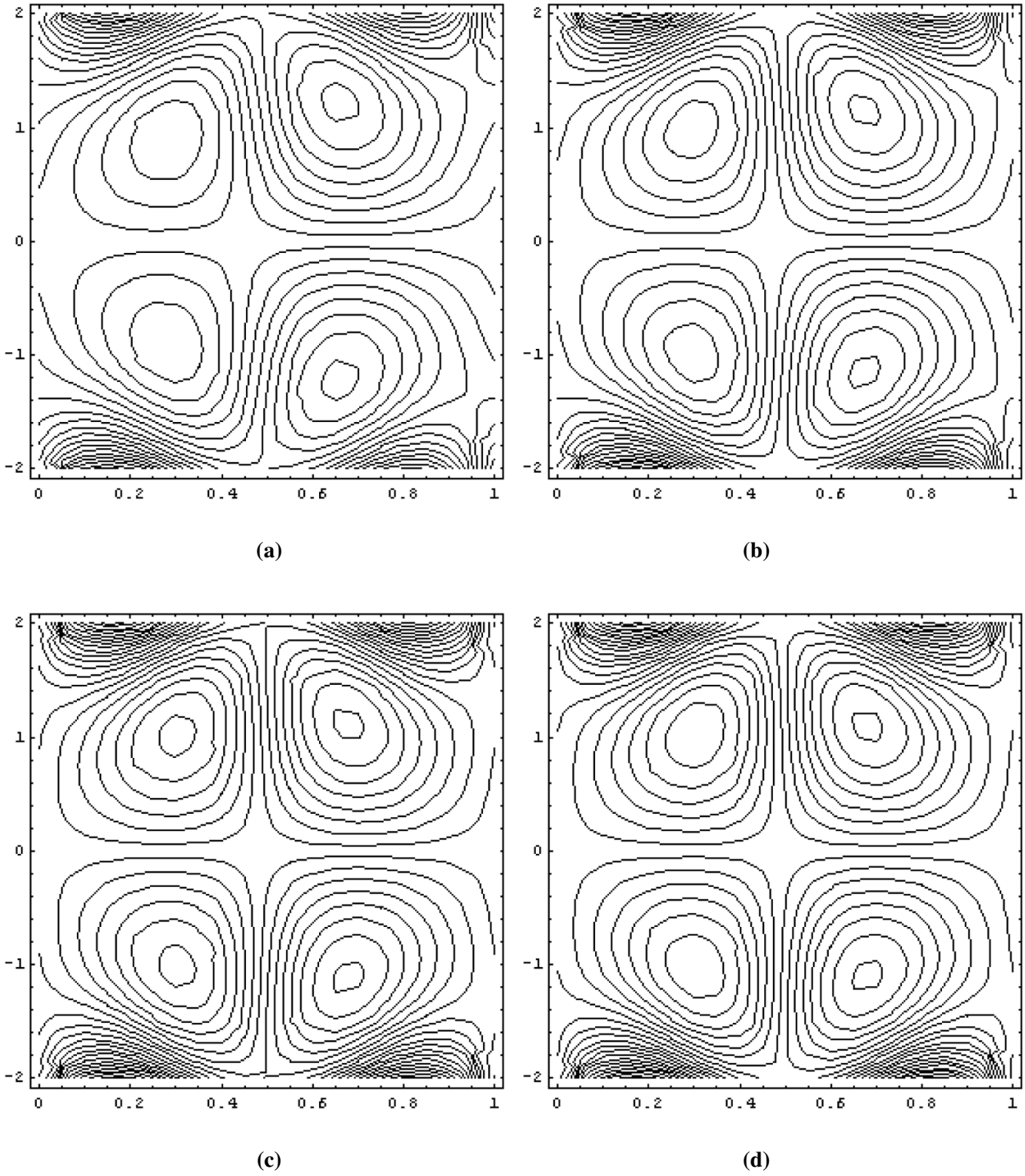

Fig. 9. Streamlines for different values of E_1: (a) for $E_1 = 0.8$, (b) for $E_1 = 1.0$, (c) for $E_1 = 1.2$, (d) for $E_1 = 1.4$. The other parameters are $y = 0.5$, $\varphi = 0.2$, $t = 0.5$, $\beta = 0.5$, $E_2 = 0.2$, $E_3 = 0.01$, $E_4 = 0.2$, $E_5 = 0.3$.

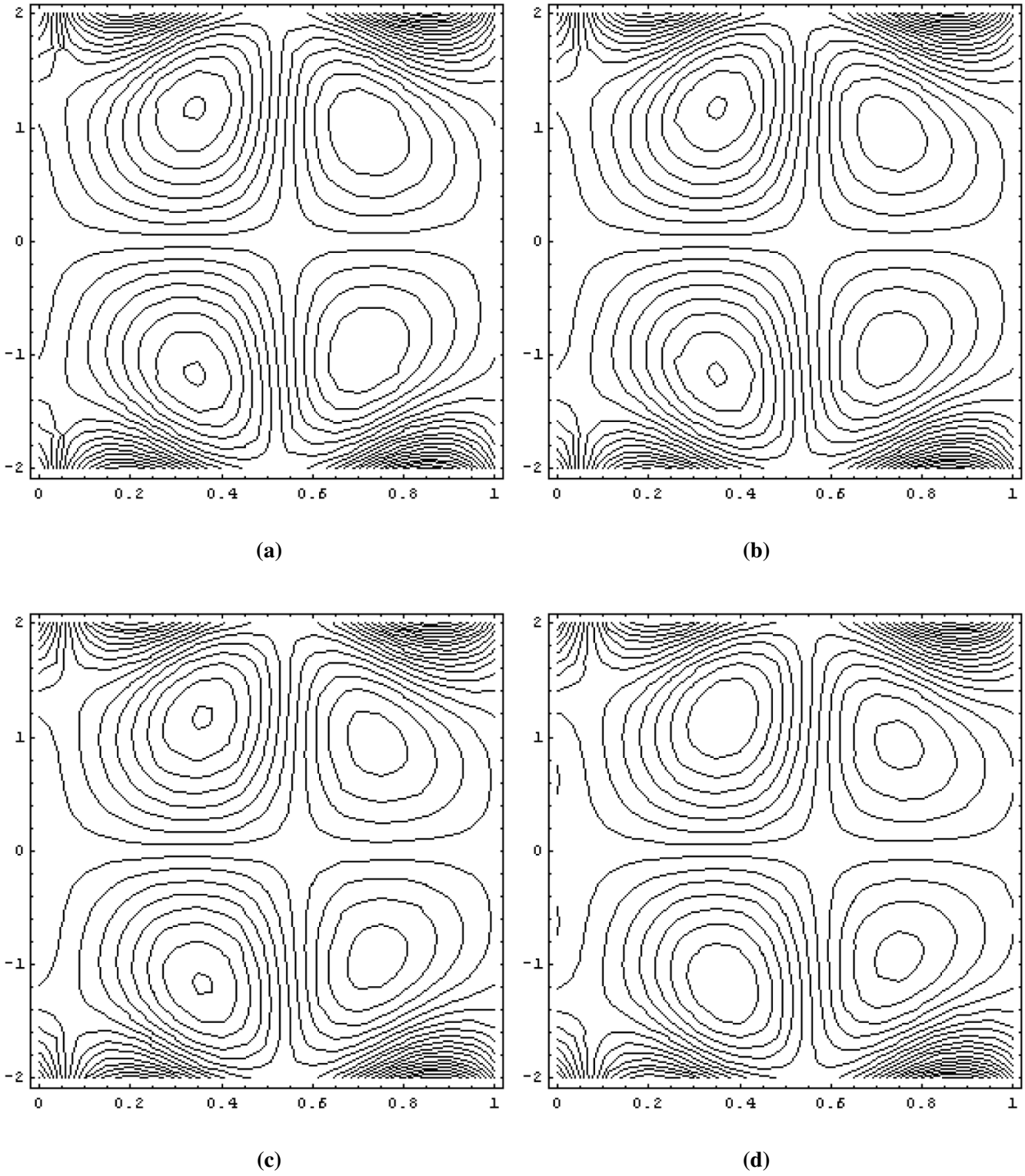

Fig. 10. Streamlines for different values of E_2: (a) for $E_2 = 0.5$, (b) for $E_2 = 0.7$, (c) for $E_2 = 0.9$, (d) for $E_2 = 1.1$. The other parameters are $y = 0.5$, $\varphi = 0.2$, $t = 0.5$, $\beta = 0.5$, $E_1 = 0.2$, $E_3 = 0.01$, $E_4 = 0.2$, $E_5 = 0.3$.

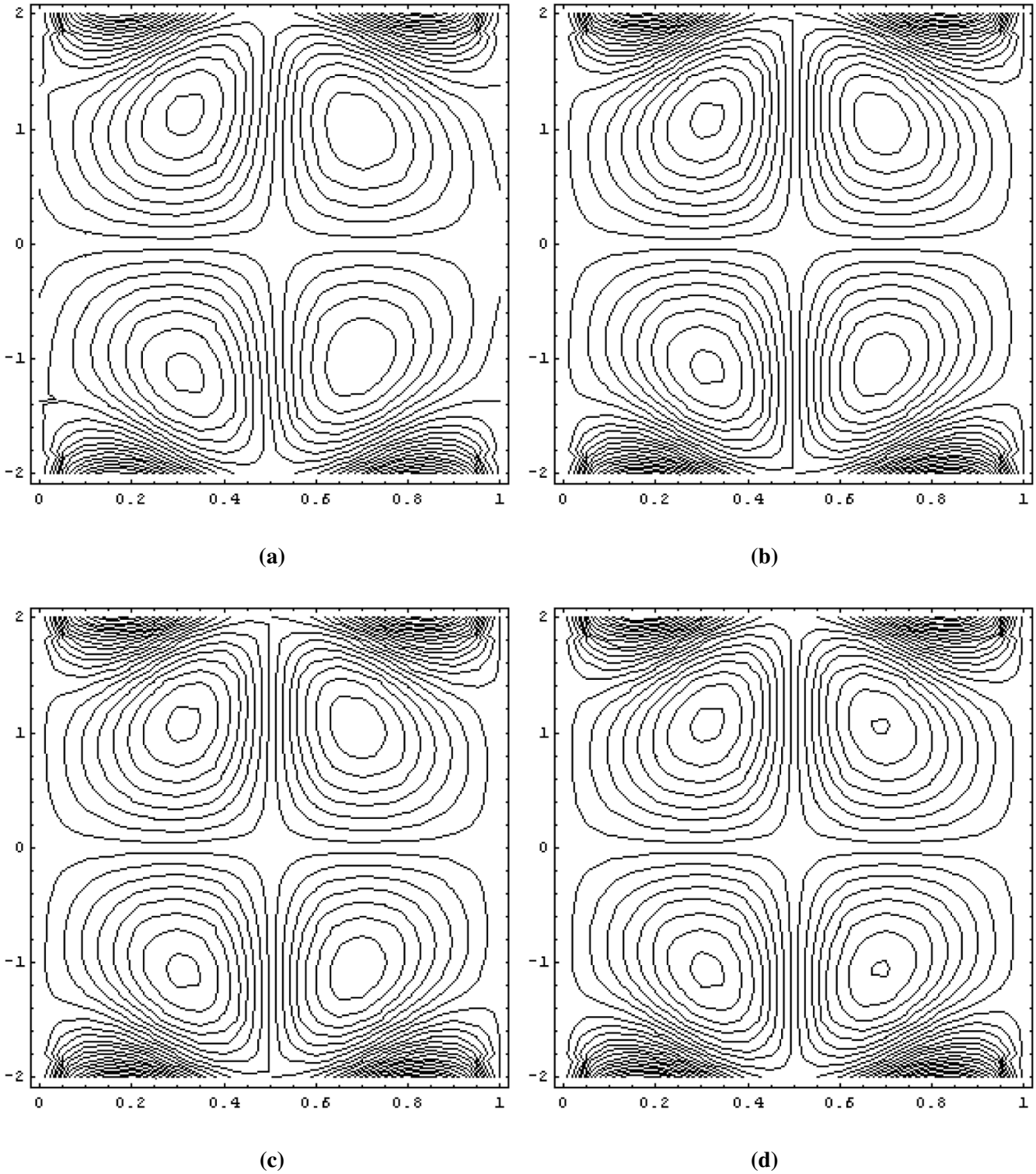

Fig. 11. Stream lines for different values of E_3, E_4 and E_5. (a) for $E_3 = 0.01$, $E_4 = 0.2$, $E_5 = 0.3$, (b) for $E_3 = 0.05$, $E_4 = 0.3$, $E_5 = 0.4$, (c) for $E_3 = 0.09$, $E_4 = 0.5$, $E_5 = 0.6$, (d) for $E_3 = 0.13$, $E_4 = 0.7$, $E_5 = 0.8$. The other parameters are $y = 0.5$, $\varphi = 0.2$, $t = 0.5$, $\beta = 0.5$, $E_1 = 0.2$, $E_2 = 0.01$.

Concluding Remarks

The theoretical study of peristaltic flow through a rectangular channel with elastic type of walls is discussed in this work. The resulting nondimensional constitutive equations are solved analytically using the eigenfunction expansion method The effects of all dimensionless physical parameters on the velocity field are computed analytically and graphically. The circulating circle/bolus phenomenon is also discussed as well. The main conclusions of the present analysis are as follows:

(1) The velocity profile decreases with increasing effects of emerging parameters β, E_1, and E_2 and reaches its maximum value at the center of the channel.

(2) The impact of variation of E_3 and E_4 on the velocity is opposite to that of β, E_1, and E_2.

(3) The number of trapping boluses decreases with increasing values of β and E_2, while the opposite behavior appears with variation of φ and E_1.

(4) It is noted that the number of trapped boluses remains the same in the left-hand side of the channel but increases in number on the right side with increasing E_3, E_4, and E_5.

REFERENCES

1. A. H. Shapiro, M. Y. Jaffrin, S. L. Weinberg, "Peristaltic pumping with long wavelengths at low Reynolds number," *J. Fluid Mech.,* **37**, 799–825 (1969).
2. T. K. Mitra and S. N. Prasad, "On the influence of wall properties and Poiseuille flow in peristalsis," *J. Biomech.,* **6**, 681–693 (1973).
3. S. Nadeem and S. Akram, "Peristaltic flow of a Williamson fluid in an asymmetric channel," *Commun. Nonlinear Sci. Numer. Simul.,* **15**, 1705–1716 (2010).
4. S. Tsangaris and N. W. Vlachakis, "Exact solution of the Navier Stokes equations for the fully developed. Pulsating flow in a rectangular duct with constant cross-sectional velocity," *ASME J. Fluids Eng.,* **125**, 382–385 (2003).
5. S. Nadeem and N. S. Akbar, "Influence of heat transfer on a peristaltic transport of a Herschel Bulkley fluid in a non-uniform tube," *Commun. Nonlinear Sci. Numer. Simul.,* **14**, 4100–4113 (2009).
6. S. Nadeem and Safia Akram, "Heat transfer in a peristaltic flow of MHD fluid with partial slip," *Commun. Nonlinear Sci. Numer. Simul.,* **15**, 312–321 (2010).
7. Kh.S. Mekheimer, "Effect of the induced magnetic field on peristaltic flow of a couple stress fluid," *Phys. Lett. A,* **372**, 4271–4278 (2008).
8. Abd El Hakeem, Abd El Naby, A.E.M. El Misiery, and I. El Shamy, "Hydromagnetic flow of generalized Newtonian fluid through a uniform tube with peristalsis," *Appl. Math. Comput.,* **173**, 856–871 (2006).
9. T. Hayat, M. Javed, and S. Asghar, *Slip Effects in Peristalsis,* Numer. Methods Partial Differ. Equ. (2011), doi:10.1002/num.20564.
10. O. Eytan and D. Elad, "Analysis of intra-uterine fluid motion induced by uterine contractions," *Bull. Math. Biol.,* **61**, 221–238 (1999).
11. M. V. Subba Reddy, M. Mishra, S. Sreenadh, and A. R. Rao, "Influence of lateral walls on peristaltic flow in a rectangular duct," *J. Fluids Eng.,* **127**, 824–827 (2005).
12. S. Nadeem and Safia Akram, "Peristaltic flow of a Jeffrey fluid in a rectangular duct," *Nonlinear Anal.: Real World Appl.,* **11**, 4238–4247 (2010).
13. S. Srinivas and M. Kothandapani, "The influence of heat and mass transfer on MHD peristaltic flow through a porous space with complaints walls," *Appl. Math. Comput.,* **213**, 197–208 (2009).